Effects of misaligning the probe beam and magnetic field in Doppler backscattering measurements

V.H. Hall-Chen[1,2], F.I. Parra[1,2], J.C. Hillesheim[2]

[1] *Rudolf Peierls Centre for Theoretical Physics, University of Oxford, Oxford OX1 3NP, UK*
[2] *CCFE, Culham Science Centre, Abingdon OX14 3DB, UK.*

Introduction

In Doppler Backscattering (DBS) measurements, the probe beam is launched into the plasma such that the beam reaches the cut-off perpendicular to the magnetic field, fulfilling the Bragg condition

$$2\mathbf{K}_b = -\mathbf{k} \simeq -\mathbf{k}_\perp. \tag{1}$$

Here $\mathbf{K}_b$ is the wavevector of the probe beam, $\mathbf{k}$ is the turbulent wavevector, and the $_\perp$ subscript represents projection perpendicular to the magnetic field. Due to the nature of turbulence in high magnetic fields, $\mathbf{k}$ is mostly perpendicular to $\mathbf{B}$. Since the Bragg condition requires $\mathbf{K}_b$ to be parallel to $\mathbf{k}$, it follows that $\mathbf{K}_b$ must be perpendicular to $\mathbf{B}$. It is difficult to meet this condition in spherical tokamaks at all points and times, hence the backscattered signal is reduced. The quantitative dependence of signal on mismatch angle is not known. Understanding this is vital for interpreting DBS data from spherical tokamaks [1].

Beam tracing

We write the electric field due to the microwaves as $\mathbf{E}e^{-i\omega t}$, where ω is the angular frequency of the microwave beam. Assuming that the electron density has equilibrium piece n_e and small fluctuating part $\delta n_e \ll n_e$, we split $\overline{\boldsymbol{\varepsilon}}$, the cold plasma dielectric tensor, into equilibrium and turbulent fluctuating parts $\overline{\boldsymbol{\varepsilon}} = \overline{\boldsymbol{\varepsilon}}_{eq} + \overline{\boldsymbol{\varepsilon}}_{tb}$, associated with probe beam $\mathbf{E}_b$ and scattered $\mathbf{E}_s$ electric fields, respectively.

We model $\mathbf{E}_b$ as a Gaussian beam, which is approximately what the DBS antenna emits. We assume that the length scale associated with the inhomogeneity L is long compared to both the width w and wavelength λ of the beam, and that the wavelength λ is much smaller than the width of the beam w, $\lambda \ll w \ll L$. We choose the specific ordering

$$\frac{w}{L} \sim \frac{\lambda}{w} \ll 1. \tag{2}$$

We then consider a region of space close to the trajectory of the central ray, $\mathbf{r} = \mathbf{q}(\tau)$, where τ is a parameter that gives the position along the ray. To define a coordinate system, we introduce the effective group velocity (this is not the true group velocity since it is a derivative with respect to the parameter τ, not with respect to time)

$$\mathbf{g} = g\hat{\mathbf{g}} = \frac{d\mathbf{q}}{d\tau}, \tag{3}$$

where $g = |\mathbf{g}|$ is the magnitude of $\mathbf{g}$, and $\hat{\mathbf{g}}$ its direction. The group velocity $\mathbf{g}$ is parallel to the central ray, and we will describe any arbitrary position as being composed of the position along $\mathbf{q}(\tau)$ and across the ray,

$$\mathbf{r} = \mathbf{q}(\tau) + \mathbf{w} = \mathbf{q}(\tau) + w_x\hat{\mathbf{u}}_x(\tau) + w_y\hat{\mathbf{u}}_y(\tau). \tag{4}$$

Here $\hat{\mathbf{u}}_x(\tau)$ and $\hat{\mathbf{u}}_y(\tau)$ are two mutually perpendicular unit vectors which are also perpendicular to $\mathbf{g}$. The unit vectors ($\hat{\mathbf{u}}_x$, $\hat{\mathbf{u}}_y$, $\hat{\mathbf{g}}$) form an orthogonal basis (Figure 1). The beam is taken to be a

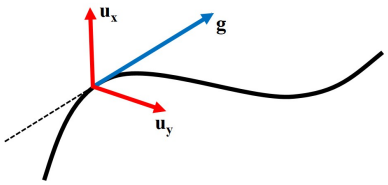

Figure 1: Beam coordinates

Gaussian envelope about a central ray. The electric field of the probe beam is

$$\mathbf{E}_b = A_{ant}\exp(i\phi_b^{(0)})\left[\frac{\det(\Im[\overline{\mathbf{\Psi}}_w])}{\det(\Im[(\overline{\mathbf{\Psi}}_{ant})_w])}\right]^{\frac{1}{4}}\sqrt{\frac{g_{ant}}{g}}\hat{\mathbf{e}}\exp\left[is+i\mathbf{K}_w\cdot\mathbf{w}+\frac{1}{2}i\mathbf{w}\cdot\overline{\mathbf{\Psi}}_w\cdot\mathbf{w}\right], \tag{5}$$

where $\phi_b^{(0)}$ is the Gouy phase of the beam, $s=\int K_g g\,d\tau$, and $\hat{\mathbf{e}}$ is the polarisation. The wavevector and position of the ray are $\mathbf{K}(\tau)$ and $\mathbf{q}(\tau)$, respectively. The curvature and width of the envelope are given by the real and imaginary parts of the 2D matrix $\overline{\mathbf{\Psi}}_w(\tau)$, respectively. We use the subscripts $_w$ and $_g$ to indicate projection perpendicular and parallel to the group velocity, respectively, while the subscript $_{ant}$ refers to the value at the antenna. The evolution of $\mathbf{g}(\tau)$, $\mathbf{K}(\tau)$, $\phi_b^{(0)}(\tau)$, and $\overline{\mathbf{\Psi}}_w(\tau)$ along the beam is given by the beam tracing equations [2].

Reciprocity

We then calculate the backscattered signal using the reciprocity theorem [3]

$$\begin{aligned}A_s = &\frac{A_{ant}g_{ant}}{2\pi i}\frac{\omega}{c}\int\frac{\sqrt{\det[\Im(\overline{\mathbf{\Psi}}_w)]}}{g}\exp(\phi_b^{(0)}+\phi_r^{(0)})\\ &\times\frac{\delta n_e}{n_e}\,\hat{\mathbf{e}}^*\cdot(\boldsymbol{\varepsilon}_{eq}-\mathbb{1})\cdot\hat{\mathbf{e}}\,\exp(2is+2i\mathbf{K}_w\cdot\mathbf{w}+i\mathbf{w}\cdot\overline{\mathbf{\Psi}}_w\cdot\mathbf{w})\,dV.\end{aligned} \tag{6}$$

Here $\phi_r^{(0)}$ is the Gouy phase of the reciprocal beam. We then order $|\mathbf{k}_\perp|\gg k_\parallel\sim L^{-1}$ and express the density perturbation as

$$\delta n_e = \int\delta N_e(\tau,\mathbf{k}_\perp)\exp\left(i\mathbf{k}_\perp\cdot\mathbf{w}+i\int\mathbf{k}_\perp\cdot\mathbf{g}\,d\tau\right)d^2k_\perp. \tag{7}$$

Writing the differential volume element as

$$dV = g\,dw_x\,dw_y\,d\tau, \tag{8}$$

we note that the integrals with respect to w_x and w_y are Gaussian integrals. Hence we get

$$\begin{aligned}\frac{A_s}{A_{ant}} = &\frac{g_{ant}}{2i}\frac{\omega}{c}\int\sqrt{\frac{\det[\Im(\overline{\mathbf{\Psi}}_w)]}{\det[\overline{\mathbf{\Psi}}_w]}}\exp(i\phi_b^{(0)}+i\phi_r^{(0)})\hat{\mathbf{e}}^*\cdot(\boldsymbol{\varepsilon}_{eq}-\mathbb{1})\cdot\hat{\mathbf{e}}\,\frac{\delta N_e}{n_e}\\ &\times\underbrace{\exp\left(2is+i\int\mathbf{k}_\perp\cdot\mathbf{g}\,d\tau\right)}_{\text{Mismatch}}\underbrace{\exp\left\{\frac{1}{4}i[2\mathbf{K}_w+(\mathbf{k}_\perp)_w]\cdot\overline{\mathbf{\Psi}}_w^{-1}\cdot[2\mathbf{K}_w+(\mathbf{k}_\perp)_w]\right\}}_{\text{Mismatch}}d\tau\,d^2k_\perp.\end{aligned} \tag{9}$$

Effect of the mismatch angle

To understand equation (9), we consider how the backscattered signal can be maximised. The $\exp(2is + i\int \mathbf{k}_\perp \cdot \mathbf{g}\, d\tau)$ piece is quickly oscillating and can be maximised using the method of stationary phase, while the $\exp\left\{\frac{1}{4}i[2\mathbf{K}_w + (\mathbf{k}_\perp)_w]\cdot\overline{\mathbf{\Psi}}_w^{-1}\cdot[2\mathbf{K}_w + (\mathbf{k}_\perp)_w]\right\}$ piece decays quickly for $2\mathbf{K}_w + (\mathbf{k}_\perp)_w \neq 0$ due to the imaginary part of $\overline{\mathbf{\Psi}}_w^{-1}$. Hence, the signal is largest when $2\frac{ds}{d\tau} + \mathbf{k}_\perp \cdot \mathbf{g} = 0$ and $2\mathbf{K}_w + (\mathbf{k}_\perp)_w = 0$, recovering the Bragg condition $2\mathbf{K}_b + \mathbf{k}_\perp = 0$ if $\mathbf{g}$ is perpendicular to $\mathbf{B}$. If they are not perpendicular, then the Bragg condition is not met in general. When there is a mismatch angle, equation (9) enables us to determine the backscattered signal. Equation (9) is a generalisation of reference [3], which assumes slab geometry.

Verification

To further understand equation (9), we study it in the limit of a conventional tokamak. In a conventional tokamak, where mismatch angle is small, we can make two approximations. First, the probe beam's path is approximately perpendicular to the magnetic field, hence $\hat{\mathbf{g}}\cdot\hat{\mathbf{b}} \simeq 0$. Second, the poloidal field B_p is small compared to the total field B. Hence, the dispersion relation of the O and X modes implies that $\mathbf{K}_w$ is small in B_p/B.

We neglect $\mathbf{K}_w$ and use the beam tracer Torbeam [2] and our post-processing code to evaluate equation (10). We choose the basis ($\hat{\mathbf{g}}$, $\hat{\mathbf{k}}_{\perp,2}$, $\hat{\mathbf{b}}$). To further simplify the equation, we assumed that δN_e does not depend on τ. This is equivalent to assuming uniform density fluctuations throughout the beam. Evaluating the integral in equation (9) with respect to $k_{\perp,2}$, we get

$$\frac{A_s}{A_{ant}} = \int I(k_{\perp,1})\ \delta N_e\left(k_{\perp,1}, k_{\perp,2}=0\right).\, dk_{\perp,1}, \tag{10}$$

Where

$$\begin{aligned} I(k_{\perp,1}) = \int \frac{g_{ant}}{in_e}\frac{\omega}{c}\sqrt{\frac{\det[\Im(\overline{\mathbf{\Psi}}_w)]}{\det[\overline{\mathbf{\Psi}}_w]}}\exp(i\phi_b^{(0)} + i\phi_r^{(0)})\hat{\mathbf{e}}^*\cdot(\varepsilon_{eq} - \mathbb{1})\cdot\hat{\mathbf{e}} \\ \times \frac{\sqrt{\pi i}}{\sqrt{\Psi_{22}^{-1}}}\exp\left(2is + ik_{\perp,1}\int g\, d\tau\right)\, d\tau. \end{aligned} \tag{11}$$

Here $\mathbf{\Psi}^{-1}$ is the inverse of $\mathbf{\Psi}_w$ and $\Psi_{22}^{-1} = \hat{\mathbf{k}}_{\perp,2}\cdot\mathbf{\Psi}^{-1}\cdot\hat{\mathbf{k}}_{\perp,2}$. We evaluate equation (11) for a tokamak with concentric circular flux surfaces (Figure 2 (a)), with a launch angle of 20°, O-mode polarisation, frequency of 55 GHz, minor radius of $a = 0.5$m, and major radius of $R_0 = 1.5$m. The poloidal and toroidal magnetic fields have the forms $B_p = B_{p,max}\left(\sqrt{(R-R_0)^2+Z^2}\right)/a$ and $B_t = B_{t,max}R_0/R$, respectively. We used $B_{p,max} = 0.01$T and $B_{t,max} = 0.67$T.

When $k_{\perp,1}$ is too small, there are no stationary points. That is, there are no points where the phase of the integrand of I is stationary (Figure 3, blue lines). Hence, the signal is suppressed (Figure 2 (b), $k_{\perp,1} > 18\text{cm}^{-1}$). When $k_{\perp,1}$ is sufficiently large, there is one stationary point (Figure 3), green lines) at the cut-off corresponding to where the Bragg condition is met. Since the beam spends more time in this region, density fluctuations here matter more than along the other sections of the beam. When $k_{\perp,1}$ is even larger, there are now two stationary points corresponding to the two points along the beam where the Bragg condition is met (Figure 3, red lines). However, the signal from these two points can interfere constructively or destructively depending on the phase difference of the waves scattered from them, explaining the oscillations in the signal when $k_{\perp,1}$ is large, as seen in Figure 2(b).

There are several reasons for the large spread of $k_{\perp,1}$ contributing to the integral in Figure 2 (b). First, the turbulence spectrum is not yet taken into account. More localisation at cut-off

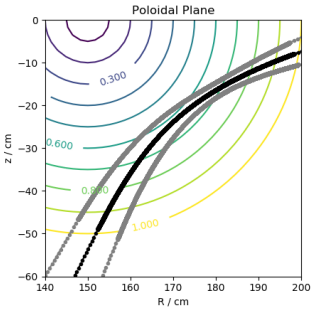

(a) Path of the beam

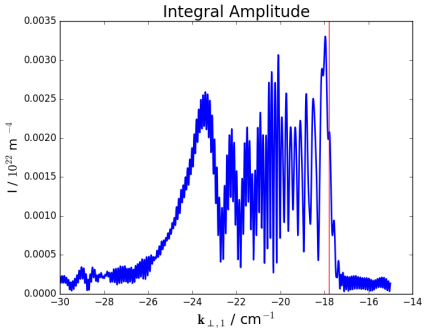

(b) Amplitude of the integral I with respect to τ, given in equation (11)

Figure 2: The black line shows the path of the beam, and the grey lines show the $1/e$ contours of the Gaussian envelope (a). The red line shows the values of $k_{\perp,1}$ where the Bragg condition is met at the cut-off (b).

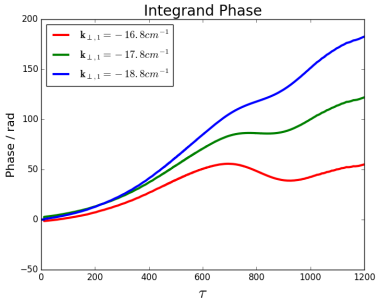

(a) Phase of the integrand in I

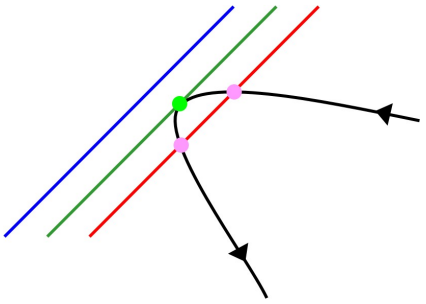

(b) Meeting the Bragg condiiton

Figure 3: The phase of the integrand as the beam propagates through the plasma (a). Schematic showing where the Bragg condition is met along the beam (b).

is expected once it is taken into account because there are more fluctuations at lower $|k_{\perp,1}|$. Second, the tokamak model is simple, with circular flux surfaces and parabolic density profiles. Third, the probe beam is launched from the outboard mid-plane with a shallow angle of 20°. Fourth, the Doppler shift would give additional localisation at the cut-off.

Conclusions

We have written a program, to be used together any beam tracing code, that is able to calculate backscattered signal in general geometry when there is no mismatch. More importantly, we have developed an analytical understanding of mismatch angle on backscattered signal, and are currently developing tools to numerically calculate effect of mismatch angle.

Acknowledgements

This work has been funded by the RCUK Energy Programme [grant number EP/P012450/1]. In order to obtain further information on the data and models underlying this work, please contact PublicationsManager@ukaea.uk. V.H. Hall-Chen's DPhil is funded by a National Science Scholarship from A*STAR, Singapore.

References

[1] J.C. Hillesheim, N.A. Crocker, W.A. Peebles, H. Meyer, A. Meakins, A.R. Field, D. Dunai, M. Carr, N. Hawkes, and MAST Team, Nuclear Fusion **55** (7), 073024 (2015)
[2] E. Poli, A.G. Peeters, and G.V. Pereverzev, Computer Physics Communications **136** (1-2), 90-104 (2001).
[3] E.Z. Gusakov, and A.V. Surkov, Plasma Physics and Controlled Fusion, **46** (7), 1143 (2004).